

LAMOST Medium-Resolution Spectral Survey of Galactic Nebulae (LAMOST MRS-N): An overview of scientific goals and survey plan

Chao-Jian Wu (武朝剑)^{1,3}, Hong Wu (吴宏)^{1,3}, Wei Zhang (张伟)^{1,3}, Juan-Juan Ren (任娟娟)^{2,3}, Jian-Jun Chen (陈建军)^{1,3}, Chih-Hao Hsia (夏志浩)⁴, Yu-Zhong Wu (吴玉中)^{1,3}, Hui Zhu (朱辉)³, Bin Li (李彬)^{5,6}, Yong-Hui Hou (侯永辉)^{7,8}, Jun-Lin Wang (王俊霖)⁴, Shuo-Ran Yu (余碩然)⁴ and LAMOST MRS Collaboration

¹ CAS Key Laboratory of Optical Astronomy, National Astronomical Observatories, Chinese Academy of Sciences, Beijing 100101, China; chjwu@bao.ac.cn

² CAS Key Laboratory of Space Astronomy and Technology, National Astronomical Observatories, Chinese Academy of Sciences, Beijing 100101, China

³ National Astronomical Observatories, Chinese Academy of Sciences, Beijing 100101, China

⁴ State Key Laboratory of Lunar and Planetary Sciences, Macau University of Science and Technology, Taipa, Macau, China

⁵ Purple Mountain Observatory, Chinese Academy of Sciences, Nanjing 210008, China

⁶ University of Science and Technology of China, Hefei 230026, China

⁷ Nanjing Institute of Astronomical Optics, & Technology, National Astronomical Observatories, Chinese Academy of Sciences, Nanjing 210042, China

⁸ School of Astronomy and Space Science, University of Chinese Academy of Sciences, Beijing 100049, China

Received 2020 July 10; accepted 2020 November 1

Abstract Since Sep. 2018, LAMOST has started the medium-resolution ($R \sim 7500$) spectral survey (MRS). We proposed the spectral survey of Galactic nebulae, including H II regions, HH objects, supernova remnants, planetary nebulae and the special stars with MRS (LAMOST MRS-N). LAMOST MRS-N covers about 1700 square degrees of the northern Galactic plane within $40^\circ < l < 215^\circ$ and $-5^\circ < b < 5^\circ$. In this 5-year survey, we plan to observe about 500 thousand nebulae spectra. According to the commissioning observations, the nebulae spectra can provide precise radial velocity with uncertainty less than 1 km s^{-1} . These high-precision spectral data are of great significance to our understanding of star formation and evolution.

Key words: surveys — ISM: general — ISM: HII regions — ISM: Herbig-Haro objects — ISM: planetary nebulae: — ISM: supernova remnants — Galaxy: disk

1 INTRODUCTION

The Milky Way is a unique laboratory for studying the formation of stars and the structure of the universe. According to the Hubble classification, the Milky Way is a typical barred spiral galaxy, which consists of disk, nuclear sphere and halo (Gerhard 2002). The Galactic plane (GP) contains the majority of baryonic matter in the Milky Way, and it is the main region of star formation and evolution. A large number of stars are born in the nebulae of the GP. The study of nebulae is of great significance to understand the formation and evolution of stars, and also the feedback of interstellar matter. Through the spectral observation of the nebulae on the GP, we can obtain the basic physical

parameters, including distance, mass, velocity, electronic temperature and density, abundance of many chemical elements, and other physical parameters of the ionized gas around the star. We can also study the physical properties of the accretion disk, accretion process of the proto-planetary disk and dynamic information. Moreover, the physical mechanism and evolution process of interstellar medium (ISM) in the early and late stages of star formation can also be studied.

However, there is not yet a complete spectral survey of emission nebulae on the GP. Large Sky Area Multi-Object fiber Spectroscopic Telescope (LAMOST), similar to Integral Field Unit (IFU) type structure, provides us with

an opportunity to make spectral observations for a large number of Galactic nebulae.

The LAMOST, also known as Guo Shou Jing Telescope, is a 4-meter effective aperture quasi-meridian reflecting Schmidt telescope, which is equipped with 4000 fibers on its 5° diameter field of view focal plane. It is the first large astronomical scientific device in China (Cui et al. 2012; Zhao et al. 2012; Wang et al. 1996; Su & Cui 2004). Until 2017, LAMOST had completed its pilot and first 5 years of low spectral resolution ($R \sim 1800$) regular sky survey, and it achieved great success.

During 2017, another new 16 medium spectral resolution ($R \sim 7500$) spectrographs were installed on LAMOST (Liu et al. 2020). The two cameras (blue and red) of each spectrograph can cover the wavelength range $4950\text{\AA} - 5350\text{\AA}$ and $6300\text{\AA} - 6800\text{\AA}$, respectively (Wu et al. 2020; Liu et al. 2020). The red part of the spectra can well cover $H\alpha$, $[\text{N II}]\lambda\lambda 6548, 6584$ and $[\text{S II}]\lambda\lambda 6717, 6731$ emission lines, while the blue part can well cover $[\text{O III}]\lambda\lambda 4959, 5007$ emission line. The six emission lines are all crucial for the Galactic nebulae.

Since Sep. 2018, LAMOST has started the second stage survey (the Medium-Resolution Spectral Survey, MRS) program. We proposed the spectral survey of Galactic nebulae with LAMOST MRS (hereafter: MRS-N). In addition to MRS-N, another several scientific goals of MRS are Galactic archaeology, stellar physics, star clusters, star formation, exoplanet and their host stars, etc.

This paper is structured as follows: Section 2 describes the proposed scientific goals. Section 3 provides a detailed report of the survey strategy, input catalog, progress and preliminary results. Finally, Section 4 gives a brief summary.

2 SCIENCE

Many works of nebulae based on LAMOST low spectral resolution have been made. LAMOST M31/M33 survey, as a part of the LAMOST Spectroscopic Survey of the Galactic Anti-center (LSS-GAC; Yuan et al. 2015), has made many efforts on nebulae, such as planetary nebulae (Yuan et al. 2010; Xiang et al. 2017; Zhang et al. 2020a) and H II regions (Wang et al. 2018; Chen et al. 2015).

The main scientific goals of our MRS-N project focus on four-type nebulae including H II regions, Herbig-Haro objects, supernovae remnants and planetary nebulae, Sabin et al. (2013) suggested that the three emission lines $H\alpha$, $[\text{S II}]$ and $[\text{N II}]$ could be used to distinguish nebulae. We aim to obtain the three-dimension (3D) properties of these nebulae such as radial velocities, velocity dispersions, reddening and oxygen abundance (Alloin et al. 1979; Pettini & Pagel 2004), which can help us to study the environments surrounding star formation regions and evolved stars and to understand the feedback

of star formation on the dynamics and energetics of Galactic interstellar medium (ISM). Compared to the low-resolution spectra, the medium resolution spectra can provide more accurate velocity measurements, and are more efficient to separate different components along the same line-of-sight of the nebulae based on their various velocity distributions.

Besides nebulae, some individual objects such as $H\alpha$ emission line stars (Hou et al. 2016), Be stars (Wu et al. 2020; Lin et al. 2015), F and OB stars (Liu et al. 2019), luminous blue variables (LBVs) (Huang et al. 2019), red supergiants (RSGs), and Wolf-Rayet stars (Zhang et al. 2020b) are also the scientific goals of our MRS-N project.

2.1 H II Regions

H II regions are the diffuse nebulae with amorphous photoionized by ultraviolet radiations emitted from young massive stars. Because the radiation sources are short-lived stars, and most of the gas are swept away by strong radiation pressure, the H II regions will fade away after a few million years (Kennicutt & Chu 1988). In addition, because the distribution of these stars and the surrounding gas are irregular, in most situation, the shape of the H II regions is far from simple Stromgren sphere, and instead they often appear clumpy and filamentary (Monreal-Ibero et al. 2011). From the optical spectra, we can easily identify strong hydrogen emission lines (such as $H\alpha$, $H\beta$) and fine-structure lines (such as $[\text{O II}]\lambda\lambda 3726, 3729$, $[\text{O III}]\lambda\lambda 4959, 5007$, $[\text{N II}]\lambda\lambda 6548, 6584$, $[\text{S II}]\lambda\lambda 6717, 6731$), which are usually used to derive current star formation rate, internal reddening, metallicities, the electron temperature and densities of the nebulae (Pérez-Montero 2017). Consequently, the H II regions are natural laboratories for studying star-forming actives and interactions between the massive stars and surrounding ISM (Mao et al. 2018).

The spatial variation of chemical abundances across the galactic disc is an observational constraint for chemical evolution models. Galactic abundance gradients in the ISM were described by Searle (1971) in a survey of H II regions in six Sc galaxies. Shaver et al. (1983) first showed that the abundances were not distributed homogeneously throughout the disk of the Milky Way. Since then radial abundance gradients probed by H II regions have been studied extensively (Simpson et al. 1995; Afflerbach et al. 1997; Deharveng et al. 2000; Esteban et al. 2005; Rudolph et al. 2006; Balser et al. 2011; Fernández-Martín et al. 2017; Esteban et al. 2017), and the results showed that the abundances were decreasing with Galactocentric distances, indicating that the inside-out models of galaxy formation are valid to explain the chemical composition of the Milky Way (Chiappini et al. 1997, 2001).

Whether the slope is uniform along the entire disc is still an open question. Some studies found that there is a flatter radial abundance gradient at the outer disc (Fich & Silkey 1991; Vilchez & Esteban 1996; Esteban et al. 2013; Korotin et al. 2014; Fernández-Martín et al. 2017), while some others did not (Deharveng et al. 2000; Rudolph et al. 2006; Esteban et al. 2017). Most recently, using H II regions in the Galactic anti-center area from LAMOST DR5 and several H II regions from the literature, Wang et al. (2018) determined the slopes of oxygen abundance gradient of inner and outer parts, and claimed the absence of flattening at the outer disc.

The Galactic plane survey of LAMOST-MRS-N is in the coverage of the Isaac Newton Telescope Photometric H-Alpha Survey of the Northern Galactic Plane (IPHAS) (Drew et al. 2005; Barentsen et al. 2014). By assigning the fibers to diffuse regions of bright H α emission, the LAMOST-MRS-N will obtain large numbers of optical spectra of H II regions on the Galactic disc, which allow us to study the radial abundance gradient and to re-check whether there is evidence of flattening at the outer disc. By comparing the results with chemical evolution models, our understanding of the formation and evolution of the Milky Way will be enhanced.

One important intrinsic characteristic of giant H II regions (diameter > 100 pc and H α luminosity $\sim 10^{39}$ erg s $^{-1}$) is that they present supersonic velocity dispersions ($\sigma \geq 12.85$ km s $^{-1}$) (Smith & Weedman 1970; Fuentes-Masip et al. 2000). There are two main kinds of possible mechanisms to explain the supersonic line widths, one is gravitational models, in which the Gaussian line profiles are assumed to be related to virialized motions within the H II regions (Terlevich & Melnick 1981); the other is wind-driven models, in which the emission line profiles are broadened by mechanical energy injected by massive stars (Dyson 1979; Tenorio-Tagle et al. 1996).

2.2 Herbig-Haro Objects

Herbig-Haro objects (HH objects, Ambartsumian 1954) are formed when narrow jets of partially ionized gas ejected by stars collide with nearby gas and dust at speeds of several hundred kilometers per second. More than 1000 individual objects have been discovered (Davis et al. 2010). They are small-scale shock regions intimately associated with star forming regions (Schwartz 1983) and can trace supersonic shock waves (Bally 2016), often found in large groups, and some can be seen around a single star, aligned with its rotational axis.

HH objects show strong hydrogen recombination lines and various forbidden lines, in particular [S II] and [O II],

but no detectable optical continuum emission. Their nature and origin remained a puzzle for some time, although it was clear from the beginning that they were somehow connected to star formation. A major step towards an understanding of HH objects came with the suggestion that their spectral properties might arise in gas that is shock excited by supersonic winds from the young stars (Schwartz 1975). The next crucial step was the discovery of the high proper motions in HH objects indicative of space motions of several hundred km s $^{-1}$ (Cudworth & Herbig 1979). Another observation led to the still widely accepted basic picture of what the majority of HH objects are: most HH objects were not independent entities (like bullets), but shock fronts in continuous, well collimated jets driven by young stellar objects (Mundt 1985, 1987).

The common methods for studying HH objects are narrow band photometry and spectral observation, while the narrow band images can provide the information of only one specific band each time. Many narrow band filters are needed to study HH objects in detail. At the same time, more observation time will be taken. Meanwhile, the spectral observations are more efficient. Fortunately, LAMOST-MRS-N provides an opportunity to study the most of the known HH objects in detail and it can identify more HH objects candidates.

2.3 Supernovae Remnants

Supernova remnants (SNRs) are the material ejected in an explosion of supernovae, which can continue their life through the interactions with the surrounding interstellar medium (ISM) for thousands or even up to a million years. SNRs are also the important sources of the injection of energy and heavy elements into the ISM, and are believed to be the possible sources of the Galactic cosmic rays. Moreover, SNRs probe the immediate surroundings of supernovae, shaped by their progenitors. SNRs are generally characterized by the interaction of supernova ejecta with the surrounding ISM. The main features of SNRs are strong shock waves, amplified magnetic field, ultra-relativistic particles (cosmic rays) generation and associated synchrotron radiation (Arbutina 2017). Currently, 294 Galactic SNRs (Green 2014) have been discovered. A great majority ($\sim 79\%$) of the known Galactic SNRs are believed to be relatively old, with ages greater than 10^3 years and radii larger than ~ 5 pc, and are evolved objects in either the adiabatic or the early radiative stages of their evolutionary development (Woltjer 1972). These old and evolved SNRs generally show characteristic shell structures (Fesen et al. 1985). About 30% of Galactic SNRs are known to have optical emission associated with their non-thermal radio emission. For old remnants,

the optical emission arises from the cooling of shocked interstellar cloud material following the passage of the remnant’s blast waves as they expand outward into the ambient medium.

Optical spectra of SNRs usually show strong emission including that of $H\alpha$, $[O\ II]\lambda\lambda\ 3726,3729$, $[O\ III]\lambda\lambda\ 4959,5007$, $[N\ II]\lambda\lambda\ 6548,6584$ and $[S\ II]\lambda\lambda\ 6717,6731$. The line intensity ratios have important physical implications. The optical spectra of SNRs have elevated $[S\ II]/H\alpha$ emission-line ratios, as compared to the spectra of normal H II regions, and through this technique, more than 1000 optical extra-Galactic SNR candidates have been detected so far (Vučićić et al. 2015). The $[S\ II]/H\alpha$ ratio can be also used to differentiate the shock-heated SNRs (ratios > 0.4 , but often considerably higher) and photoionized nebulae (0.4, but typically < 0.2). As in typical H II regions, sulfur exists mainly in the form of $[S\ III]$, thus the $[S\ III]/H\alpha$ ratio is very low. While after the shock wave from an SN explosion has propagated through the surrounding medium, and the material has cooled sufficiently, a variety of ionization states can be present, including the $[S\ II]$, thus leading to the increased ratio $[S\ II]/H\alpha$ observed in SNRs (Blair & Long 2004). Generally, in H II regions the material is too ionized to produce forbidden lines of $[O\ I]$, $[N\ II]$ or $[S\ II]$, while in SNRs, both the models of Allen et al. (2008) and observations show optical spectra containing these forbidden lines (Long 2016). Furthermore, the $[S\ II]6717/[S\ II]6731$ ratio is electron density sensitive, thus can be used to obtain the electron density. The $H\alpha/[N\ II]6584$ ratio is a widely used tool for investigating nitrogen-to-hydrogen abundance variations among SNRs. Thus it is important to obtain complete sampling of the optical spectra covering these emissions in SNRs.

Although several large and evolved SNRs have been well studied morphologically in the optical, only a limited amount of spectroscopic data are available for those faint optical remnants, especially for those with large angular sizes. While many SNRs are very large, where there are 10 large SNRs with angular sizes greater than 2° (Orchiston et al. 2015), it would be extremely time consuming to obtain spectra covering such a large spatial extent using regular telescopes. The wide field of view, multi-fiber survey telescope LAMOST thus serves as a perfect tool for mapping the details of those extremely extended SNRs. Ren et al. (2018) has tried to map a large SNR (the S147 with angular diameter ~ 200 arcmin) with the LAMOST low-resolution ($R\sim 1800$) spectra, but due to the low-resolution, the details cannot be mapped clearly. With this increased higher resolution of MRS-N, more detailed emission features and kinematics properties can be mapped for SNRs, thus leading to better understandings of the properties of SNRs.

2.4 Planetary Nebulae

Planetary nebulae (PNe) were originally thought to be members of H II regions. In fact, they are completely different from normal emission nebulae. PNe are the evolutionary end products of low- and intermediate-mass stars ($1 \sim 8 M_\odot$). The total number of Galactic PNe is about 2860, including ~ 1500 in the Galactic PN Catalogue of Kohoutek (2001), ~ 1200 PNe listed in the Macquarie-AAO-Strasbourg $H\alpha$ Catalogue of Galactic PNe (MASH; Parker et al. 2006; Miszalski et al. 2008), and ~ 160 faint extended PNe discovered by the IPHAS. Most PNe are located close to the Galactic plane and suffer larger interstellar extinction. They always show low surface brightness and can be easily mixed with background diffuse nebulae or star formation regions.

With the great help of MRS-N, a significant fraction of known PNe ($\sim 14\%$; 400 PNe) will be observed for studying their 3D ionized structures based on various nebular expansion velocities. The gaseous structures of Galactic PNe and surrounding nebulae are easily separated by their various spatial expansion velocities. In addition, some foundational properties of these PNe can also be derived. The survey provides us with an opportunity to study 3D ionized structures and electron density distributions of Galactic PNe, the evolution of various morphological PNe, and the chemical abundance of our galaxy.

MRS with large spatial coverage and high sensitivity as a powerful tool to study PNe obscured in the GP. Many new PNe are expected to discover through this survey, containing young, compact PNe and old, extended, faint PNe. The nature and the PN status of these nebulae can be identified using the $\log(H\alpha/[N\ II])$ vs. $\log(H\alpha/[S\ II])$ emission-line-ratio diagnostic diagram (Hsia & Zhang 2014), which is a useful probe to distinguish PNe from H II regions and SNRs with ionized gaseous nebulae.

3 SURVEY PLAN

3.1 Strategy

Most nebulae are located on the GP. So the survey areas of MRS-N mainly cover the northern GP. The northern GP is within the Galactic longitude range $40^\circ < l < 215^\circ$ and the latitude range $-5^\circ < b < 5^\circ$, totally about 1700 square degrees. Furthermore, four large size nebulae are selected to be observed with MRS as the specific areas in our galaxy. The four specific areas are Westerhout 5 (H II region, hereafter West), Rosette Nebula+NGC2264 (H II region, hereafter Ros), Cygnus Loop (SNRs, hereafter Cyg) and Simeis 147 (SNRs, hereafter S147), respectively.

In MRS-N, we plan to use 123 plates cover the GP areas (blue circles in Fig. 2). Figure 2 shows that the MRS-

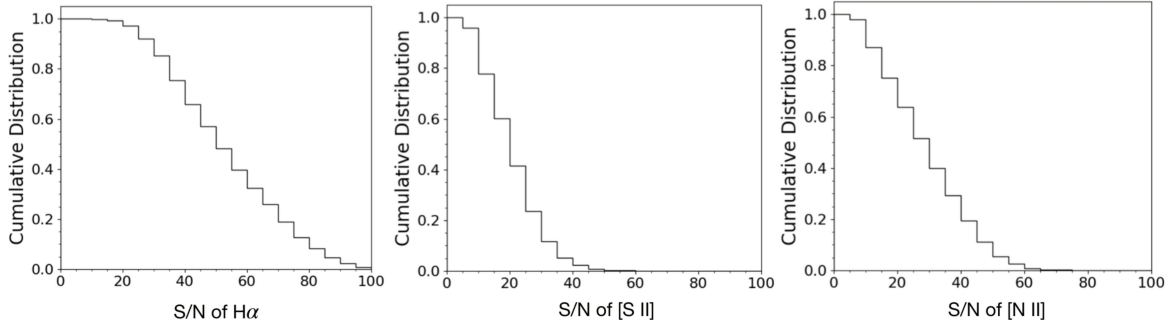


Fig. 1 The distribution of S/N ratio of H α , [S II] and [N II]. It is clearly to see that the emission lines with S/N greater than 10 make up nearly 80% of the total.

N coverage can cover most of H II region and SNRs in the northern celestial sphere. A plate, covering about 20 deg² (a circle with a diameter of 5°), is defined by MRS team as continuously taking three single 1200 s (900 s for MRS) exposure and obtain the co-added spectra with total exposure time of 3×1200 s (3×900 s for MRS-N). Figure 1 shows the distribution of signal-to-noise (S/N) ratio of H α , [S II] and [N II] from one plate. The emission lines with S/N greater than 10 make up nearly 80% of the total. So the 900 s exposure time of MRS-N can provide enough high S/N ratio nebulae spectra.

We plan to use 10 circles with a diameter of 5° (hereafter: 5d-circle) to cover the four specific areas (1 5d-circle for S147, 2 for West, 2 for Cyg and 5 for Ros). The exposure time of each 5d-circle is designed as 16 × 900 s (red circles in Fig. 2).

Finishing the 123 plates and 10 5d-circles, a total of 500 thousand nebulae spectra will take 132.25 hours. MRS-N will be assigned 30 hours per year (150 h for 5 years). Consequently, we could finish the MRS-N survey within 5 years without considering other objective factors, such as the weather.

The commissioning observations were carried out on 2018 Mar. 4-5. Figure 3 (a) shows the fiber distribution. More detailed observation information are listed in Table 1. The results showed that MRS-N is seriously affected by the moonlight. The spectrum of one fiber (red plus in Fig. 3(b)) is presented in Figure 4. The H α absorption and emission line at 6563 Å are obviously mixed together. However, the absorption lines are not visible at [N II]($\lambda\lambda$ 6548,6584) and [S II]($\lambda\lambda$ 6717,6731). In fact, the H α absorption line comes from the moonlight; to be more exact, from the sunlight. On closer examination, we found that the spectrum was no longer affected when the altitude of the moon was lower than 1°. So all the observation time of MRS-N should be assigned into a time range before the moon rises or after the moon sets. This will cause the observation time of MRS-N to be very urgent, which is why we adjust the sub-exposure time to 900s.

Table 1 The Commissioning Observation of MRS-N

Date	Time (UT)	Exposure (s)	Alt of Moon
2018-03-04	13:19:32	900	+6.5°
2018-03-05	13:01:53	900	−8°

3.2 Input Catalog

The input catalog is very important to LAMOST, because it can be used to allocate the fiber’s coordinates. MRS-N mainly focus on the spectra of non-point source (such as the structure of nebulae). However, there is not yet a catalog containing the structure of nebulae. Therefore, the input catalogs of MRS-N should be made independently unlike other MRS projects.

The input catalogs of four specific areas are made by comparing with optical images from the Digitized Sky Survey (DSS) and Narrow Band Survey (NBS). From optical images, some bright stars, some sky areas and the positions of interesting structure of nebulae are selected to compose input catalogs.

The input catalog of GP area is very complex. We divide the northern GP area into about 1.5 million 2′×2′ grids. Each grid can be considered as the moving area of each fiber. Then we cross-match the 1.5 million grids with Hipparcos main catalog and Pan-STARRS1 (PS1). If a star within a grid is brighter than 13 mag (*r* band), then the star is selected as location of fiber with objtype *STAR*. By comparing with IPHAS and NBS images, if a star within a grid is bright than 18 mag and fainter than 13 mag, then the location of fiber within the same grid should avoid the star with objtype *skylight* or *NEB* (Nebulae). Else, if there is no star in a grid or the star is too faint to be observed, then the location of fiber should be pointed to the brightest position with objtype *NEB* within the grid (Fig. 5). In addition, we integrated some F stars, OB stars and emission stars from IPHAS into the input catalog of GP area.

Eventually, we finished a complete input catalog of MRS-N with more than 1.5 million coordinates.

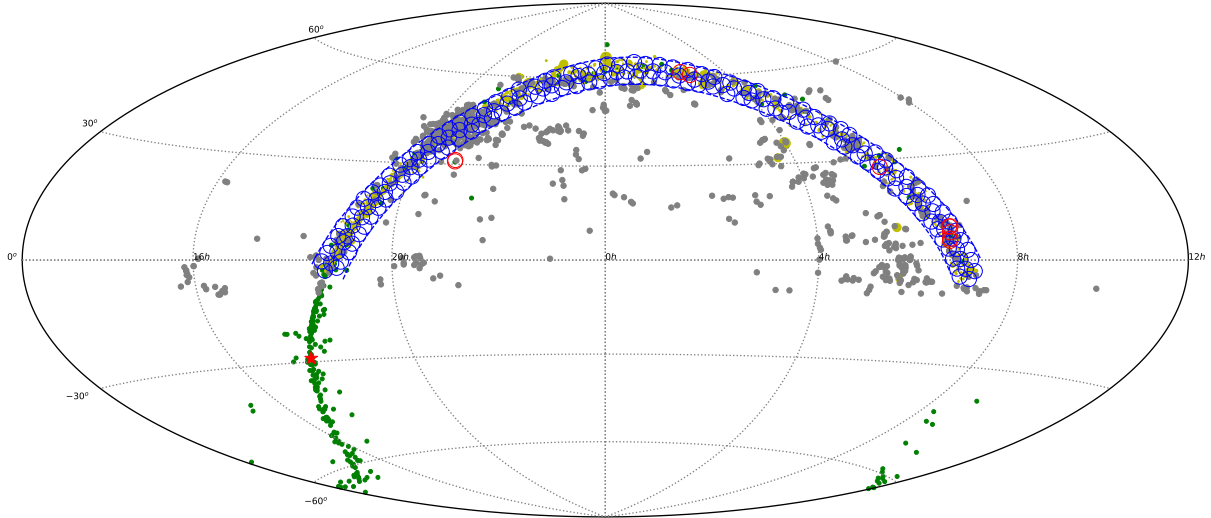


Fig. 2 123 GP plates (*blue circles*) and four specific plates (*red circles*) for MRS-N in an Equatorial Aitoff projection. Most of the bright nebulae in the Milky Way are marked with gray dots. The green dots represent the SNRs and the gray ones represent the H II region. The red star is the location of the Galactic center.

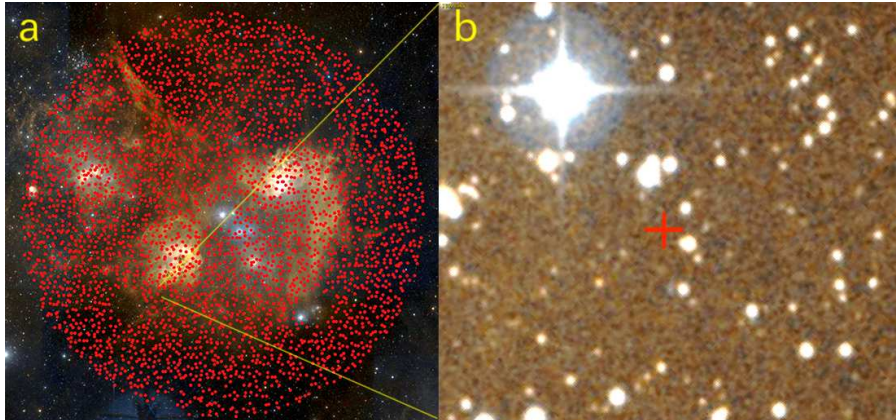


Fig. 3 (a): Fiber distribution of the commissioning observation on 2018 Mar. 4. (b): One fiber pointing to the nebula, whose spectrum is drawn in Fig. 4.

3.3 Data Description and Preliminary Results

The data processing of MRS-N is different from LAMOST 1D pipeline (Luo et al. 2012, 2015). LAMOST 1D pipeline gives the physical parameters after deducting the skylight background. However, the method of deducting skylight background is not applicable to the nebulae spectra. How to reduce the skylight in the spectra of the nebulae is still under study. Therefore, MRS-N needs to have its own pipeline. The original nebulae spectra we get are the 1D spectra given by LAMOST 2D pipeline. The process includes dark and bias subtraction, flat field correction, spectral extraction, the first wavelength calibration. The MRS-N pipeline developed by MRS-N

team includes deduction of cosmic rays, merging sub-exposures, fitting skylight emission line, reducing skylight background (optional), secondary wavelength calibration and parameters measurement of nebular emission line (such as radial velocity, intensity ratio of emission line, relative flux, line width, intensity and so on). More details about pipeline, data processing and data release will be presented in Wu et al. (2020 in prep).

Due to the more complex data processing, the data release of MRS-N is one year later than that of LAMOST. According to the LAMOST data release policy, the official data release has a protection period of 18 months. That is to say, the nebulae spectra of first year (from the second half of 2018 to the first half of 2019) will be officially released

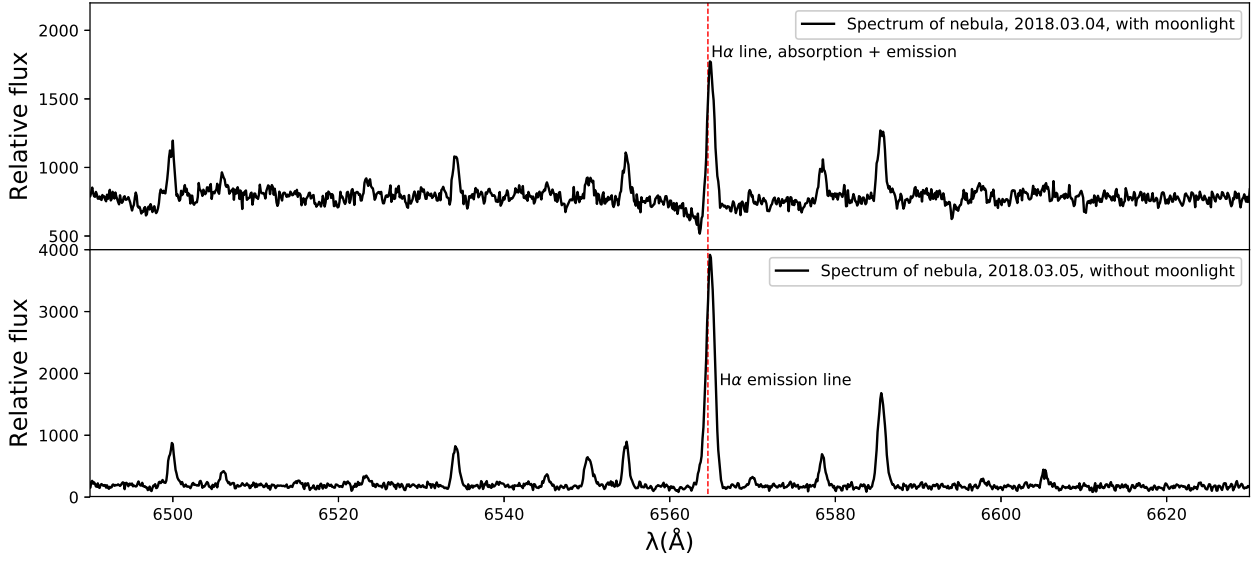


Fig. 4 Two spectra of commissioning observation. The upper panel shows a nebula spectrum observed on 2018 Mar. 4, when the moon had already risen. It is clearly to see that the $H\alpha$ absorption and emission lines at 6563 \AA were mixed together. The bottom panel shows the nebula spectrum observed on 2018 Mar. 5, before the moon rose.

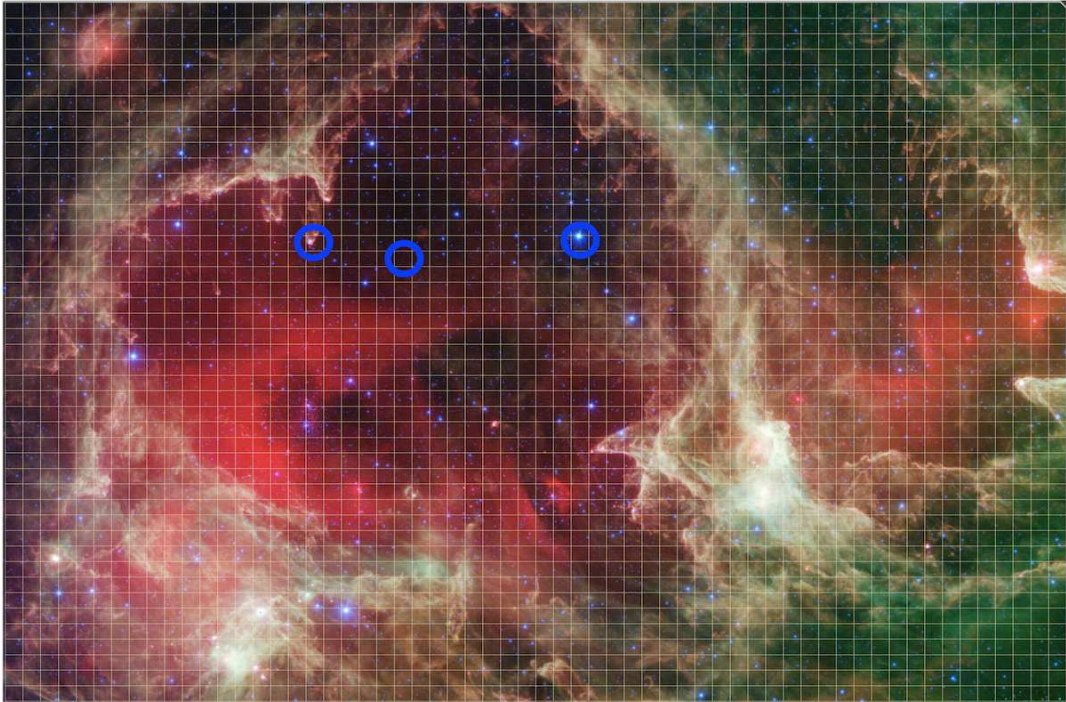


Fig. 5 Creating the input catalog of MRS-N. The size of each grid is $2' \times 2'$. If a star within a grid is brighter than 13 magnitude (r band), then the star is selected as location of fiber (*right blue circle*), else if there is no star in a grid or the star is too faint to observe, then the location of fiber will be pointed to the brightest position (*left and middle blue circle*). The background image is Westerhout 5.

in March 2021, and the rest will be done in the same manner. It is important to note that the nebulae spectra in LAMOST DR7 has been processed by subtracting the skylight background and the results are not up to the release standard of MRS-N. If someone wants to use

the nebulae spectra for science, they should use the data released by MRS-N.

Figures 6, 7 and 8 are the red part nebulae spectra observed on 2018 Mar. 5, which show three various $H\alpha$ emission lines composited with different components. The double and multiple components may be the result of the

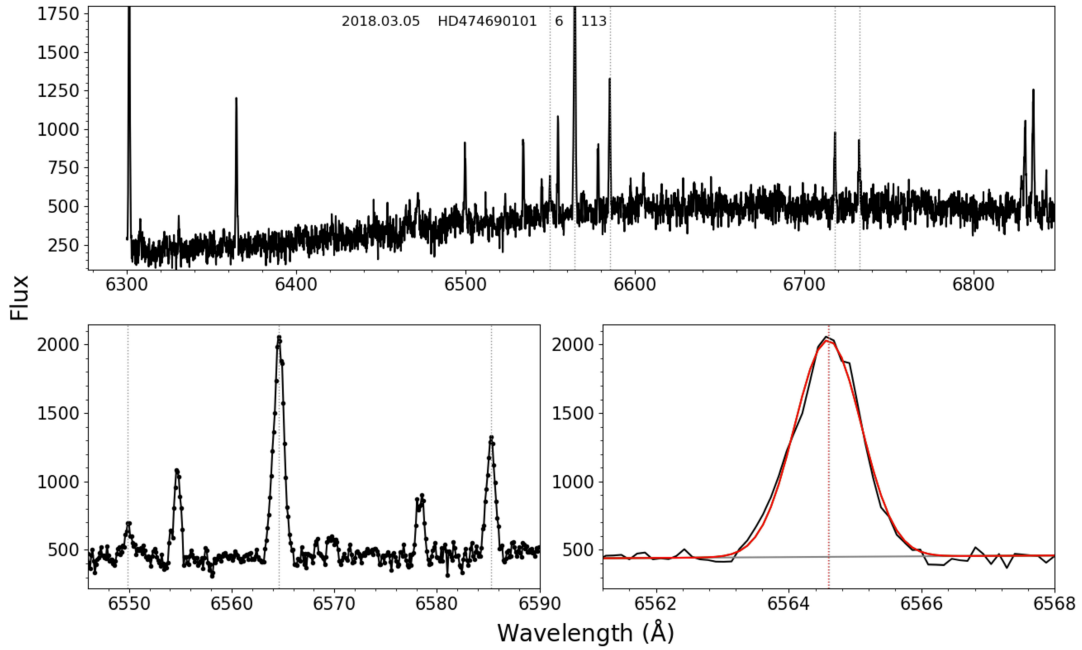


Fig. 6 H α emission line of nebulae with single-component.

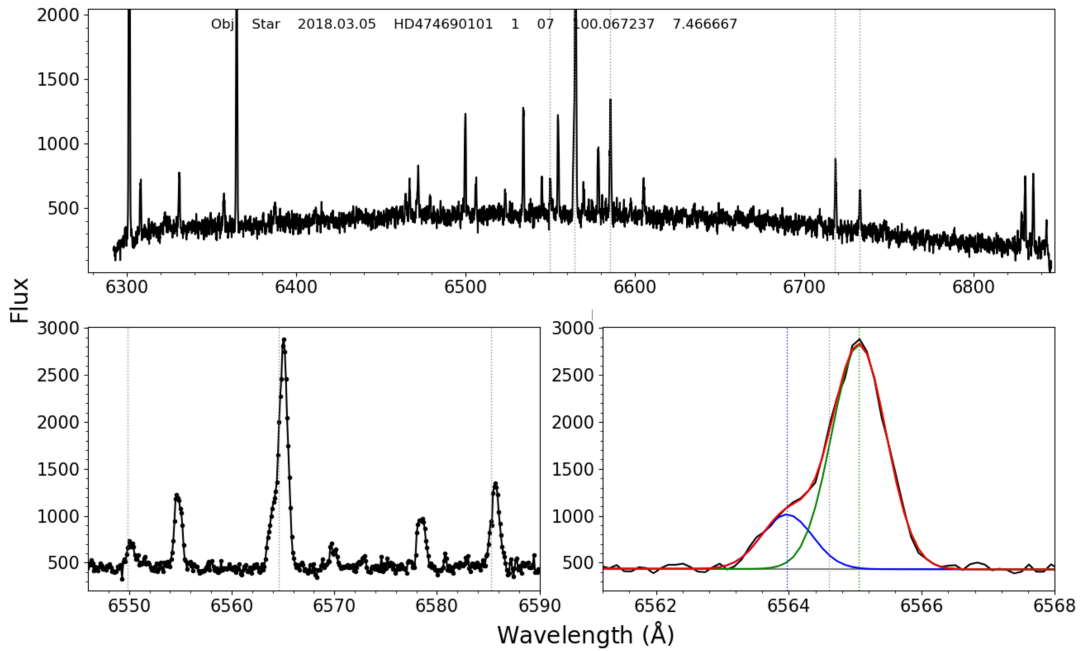


Fig. 7 H α emission line of nebulae with double-component.

emissions produced by the nebulae with various expansion velocities along the line of sight.

Ren et al. (2020) investigated the precision of wavelength calibration and found that there are systematic deviations of radial velocities (RVs) from ~ 0.1 to

4 km s^{-1} for different plates. After fitting seven sky emission lines in the red part of MRS to recalibrate the wavelength, the precision of RVs is less than 1 km s^{-1} . All of the future MRS-N data will be recalibrated with this method.

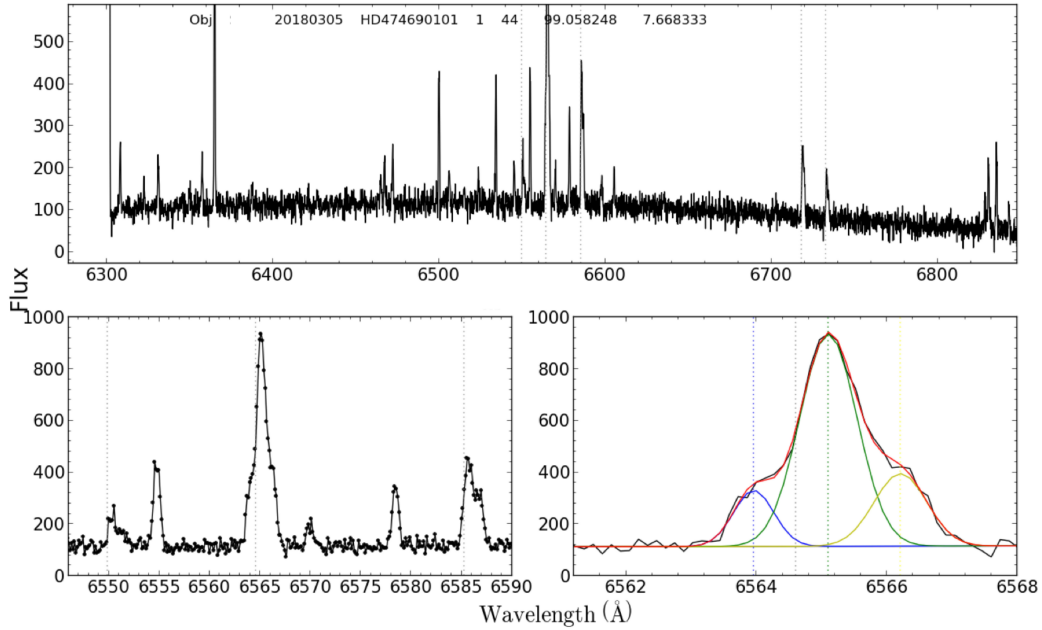


Fig. 8 $H\alpha$ emission line of nebulae with multi-component.

4 SUMMARY

As the first large optical astronomical scientific device in China, LAMOST has achieved great success for the first stage of low-resolution spectroscopic survey. Since Sep. 2018, LAMOST has started to conduct medium-resolution spectroscopic survey and will significantly increase the number of stellar and nebulae spectra with medium-resolution. As a sub-project of MRS, we proposed the spectral survey of Galactic nebulae with MRS. In MRS-N, the RVs, velocity dispersions, reddening and chemical compositions of most nebulae on the northern GP can be studied. Now, MRS-N has completed its two-year observation plan, which is the current largest nebulae survey over the world. In this paper, the detailed scientific goals and survey plan are presented. The first data release of MRS-N is scheduled for the third quarter of 2020 (Wu et al. 2020, in prep).

Acknowledgements This project is supported by the National Natural Science Foundation of China (Grant Nos. 12073051, 12090040, 12090041, 11733006, 11403061, 11903048, U1631131, 11973060, 12090044, 12073039, 11633009, U1531118, 11403037, 11225316, 11173030, 11303038, Y613991N01, U1531245 and 11833006), and the Key Laboratory of Optical Astronomy, National Astronomical Observatories, Chinese Academy of Sciences, and the Key Research Program of Frontier Sciences, CAS (Grant No. QYZDY-SSW-SLH007).

C.-H. Hsia acknowledges the supports from the Science and Technology Development Fund, Macau SAR

(file No. 0007/2019/A) and Faculty Research Grants of the Macau University of Science and Technology (No. FRG-19-004-SSI).

Guo Shou Jing Telescope (the Large Sky Area Multi-Object Fiber Spectroscopic Telescope LAMOST) is a National Major Scientific Project built by the Chinese Academy of Sciences. Funding for the project has been provided by the National Development and Reform Commission. LAMOST is operated and managed by the National Astronomical Observatories, Chinese Academy of Sciences.

References

- Afflerbach, A., Churchwell, E., & Werner, M. W. 1997, *ApJ*, 478, 190
- Allen, G. E., Houck, J. C., & Sturmer, S. J. 2008, *ApJ*, 683, 773
- Alloin, D., Collin-Souffrin, S., Joly, M., & Vigroux, L. 1979, *A&A*, 78, 200
- Ambartsumian, V. A. 1954, in *Liege International Astrophysical Colloquia*, 5, 293
- Arbutina, B. 2017, *Publications de l’Observatoire Astronomique de Beograd*, 97, 1
- Bally, J. 2016, *ARA&A*, 54, 491
- Balser, D. S., Rood, R. T., Bania, T. M., et al. 2011, *ApJ*, 738, 27
- Barentsen, G., Farnhill, H. J., Drew, J. E., et al. 2014, *MNRAS*, 444, 3230
- Blair, W. P., & Long, K. S. 2004, *ApJS*, 155, 101
- Chen, B.-Q., Liu, X.-W., Xiang, M.-S., et al. 2015, *RAA (Research in Astronomy and Astrophysics)*, 15,

- 1392
- Chiappini, C., Matteucci, F., & Gratton, R. 1997, *ApJ*, 477, 765
- Chiappini, C., Matteucci, F., & Romano, D. 2001, *ApJ*, 554, 1044
- Cudworth, K. M., & Herbig, G. 1979, *AJ*, 84, 548
- Cui, X.-Q., Zhao, Y.-H., Chu, Y.-Q., et al. 2012, *RAA (Research in Astronomy and Astrophysics)*, 12, 1197
- Davis, C. J., Gell, R., Khanzadyan, T., et al. 2010, *A&A*, 511, A24
- Deharveng, L., Peña, M., Caplan, J., & Costero, R. 2000, *MNRAS*, 311, 329
- Drew, J. E., Greimel, R., Irwin, M. J., et al. 2005, *MNRAS*, 362, 753
- Dyson, J. E. 1979, *A&A*, 73, 132
- Esteban, C., Carigi, L., Copetti, M. V. F., et al. 2013, *MNRAS*, 433, 382
- Esteban, C., Fang, X., García-Rojas, J., et al. 2017, *MNRAS*, 471, 987
- Esteban, C., García-Rojas, J., Peimbert, M., et al. 2005, *ApJL*, 618, L95
- Fernández-Martín, A., Pérez-Montero, E., Vílchez, J. M., & Mampaso, A. 2017, *A&A*, 597, A84
- Fesen, R. A., Blair, W. P., & Kirshner, R. P. 1985, *ApJ*, 292, 29
- Fich, M., & Silkey, M. 1991, *ApJ*, 366, 107
- Fuentes-Masip, O., Muñoz-Tuñón, C., Castañeda, H. O., et al. 2000, *AJ*, 120, 752
- Gerhard, O. 2002, *Space Sci. Rev.*, 100, 129
- Green, D. A. 2014, in *Supernova Environmental Impacts*, ed. A. Ray & R. A. McCray, 296, 188
- Hou, W., Luo, A. L., Hu, J.-Y., et al. 2016, *RAA (Research in Astronomy and Astrophysics)*, 16, 138
- Hsia, C.-H., & Zhang, Y. 2014, *A&A*, 563, A63
- Huang, Y., Zhang, H. W., Wang, C., et al. 2019, *ApJL*, 884, L7
- Kennicutt, Robert C., J., & Chu, Y.-H. 1988, *AJ*, 95, 720
- Kohoutek, L. 2001, *A&A*, 378, 843
- Korotin, S. A., Andrievsky, S. M., Luck, R. E., et al. 2014, *MNRAS*, 444, 3301
- Lin, C.-C., Hou, J.-L., Chen, L., et al. 2015, *RAA (Research in Astronomy and Astrophysics)*, 15, 1325
- Liu, C., Fu, J., Shi, J., et al. 2020, *arXiv e-prints*, arXiv:2005.07210
- Liu, Z., Cui, W., Liu, C., et al. 2019, *ApJS*, 241, 32
- Long, K. 2016, *What Makes Radio-detected and Optically-detected Supernova Remnants in NGC6946 Different?*, *HST Proposal*
- Luo, A. L., Zhang, H.-T., Zhao, Y.-H., et al. 2012, *RAA (Research in Astronomy and Astrophysics)*, 12, 1243
- Luo, A. L., Zhao, Y.-H., Zhao, G., et al. 2015, *RAA (Research in Astronomy and Astrophysics)*, 15, 1095
- Mao, Y.-W., Lin, L., & Kong, X. 2018, *ApJ*, 853, 151
- Miszalski, B., Parker, Q. A., Acker, A., et al. 2008, *MNRAS*, 384, 525
- Monreal-Ibero, A., Relaño, M., Kehrig, C., et al. 2011, *MNRAS*, 413, 2242
- Mundt, R. 1985, *The Observatory*, 105, 224
- Mundt, R. 1987, *Mitteilungen der Astronomischen Gesellschaft Hamburg*, 70, 100
- Orchiston, W., Green, D. A., & Strom, R. 2015, *New Insights From Recent Studies in Historical Astronomy: Following in the Footsteps of F. Richard Stephenson*, 43 (Springer International Publishing Switzerland)
- Parker, Q. A., Acker, A., Frew, D. J., et al. 2006, *MNRAS*, 373, 79
- Pérez-Montero, E. 2017, *PASP*, 129, 043001
- Pettini, M., & Pagel, B. E. J. 2004, *MNRAS*, 348, L59
- Ren, J.-J., Liu, X.-W., Chen, B.-Q., et al. 2018, *RAA (Research in Astronomy and Astrophysics)*, 18, 111
- Ren, J.-J., Wu, H., Wu, C.-J., et al. 2020, *arXiv e-prints*, arXiv:2008.06236
- Rudolph, A. L., Fich, M., Bell, G. R., et al. 2006, *ApJS*, 162, 346
- Sabin, L., Parker, Q. A., Contreras, M. E., et al. 2013, *MNRAS*, 431, 279
- Schwartz, R. D. 1975, *ApJ*, 195, 631
- Schwartz, R. D. 1983, *RMxAA*, 7, 27
- Searle, L. 1971, *ApJ*, 168, 327
- Shaver, P. A., McGee, R. X., Newton, L. M., Danks, A. C., & Pottasch, S. R. 1983, *MNRAS*, 204, 53
- Simpson, J. P., Colgan, S. W. J., Rubin, R. H., et al. 1995, *ApJ*, 444, 721
- Smith, M. G., & Weedman, D. W. 1970, *ApJ*, 161, 33
- Su, D.-Q., & Cui, X.-Q. 2004, *ChJAA (Chin. J. Astron. Astrophys.)*, 4, 1
- Tenorio-Tagle, G., Muñoz-Tunon, C., & Cid-Fernandes, R. 1996, *ApJ*, 456, 264
- Terlevich, R., & Melnick, J. 1981, *MNRAS*, 195, 839
- Vílchez, J. M., & Esteban, C. 1996, *MNRAS*, 280, 720
- Vučetić, M. M., Ćiprijanović, A., Pavlović, M. Z., et al. 2015, *Serbian Astronomical Journal*, 191, 67
- Wang, L.-L., Luo, A. L., Hou, W., et al. 2018, *PASP*, 130, 114301
- Wang, S.-G., Su, D.-Q., Chu, Y.-Q., et al. 1996, *Appl. Opt.*, 35, 5155
- Woltjer, L. 1972, *ARA&A*, 10, 129
- Wu, C.-J., Wu, H., Hsia, C.-H., et al. 2020, *RAA (Research in Astronomy and Astrophysics)*, 20, 033
- Xiang, M., Liu, X., Zhang, M., et al. 2017, in *Planetary Nebulae: Multi-Wavelength Probes of Stellar and Galactic Evolution*, eds. X. Liu, L. Stanghellini, & A. Karakas, 323, 388
- Yuan, H.-B., Liu, X.-W., Huo, Z.-Y., et al. 2010, *RAA (Research in Astronomy and Astrophysics)*, 10, 599
- Yuan, H. B., Liu, X. W., Huo, Z. Y., et al. 2015, *MNRAS*, 448, 855
- Zhang, M., Chen, B.-Q., Huo, Z.-Y., et al. 2020a, *RAA (Research in Astronomy and Astrophysics)*, 20, 097
- Zhang, W., Todt, H., Wu, H., et al. 2020b, *ApJ*, 902, 62
- Zhao, G., Zhao, Y.-H., Chu, Y.-Q., et al. 2012, *RAA (Research in Astronomy and Astrophysics)*, 12, 723